













All-optical magnetization switching of GdFe by double-pulse laser excitation

Rahil Hosseinifar, Felix Steinbach, Ivar Kumberg, José Miguel Lendínez, Sangeeta Thakur, Sebastien E. Hadjadj, Jendrik Gördes, Chowdhury S. Awsaf, Mario Fix, Manfred Albrecht, Florian Kronast, Unai Atxitia, Clemens von Korff Schmising, Wolfgang Kuch

Angaben zur Veröffentlichung / Publication details:

Hosseinifar, Rahil, Felix Steinbach, Ivar Kumberg, José Miguel Lendínez, Sangeeta Thakur, Sebastien E. Hadjadj, Jendrik Gördes, et al. 2025. "All-optical magnetization switching of GdFe by double-pulse laser excitation." *Physical Review B* 112 (17): 174406.
<https://doi.org/10.1103/h8j7-4f2z>.

All-optical magnetization switching of GdFe by double-pulse laser excitation

Rahil Hosseinifar ¹, Felix Steinbach,² Ivar Kumberg ¹, José Miguel Lendínez ³, Sangeeta Thakur ¹,
Sebastien E. Hadjadj ¹, Jendrik Gördes ¹, Chowdhury S. Awsaf ¹, Mario Fix,⁴ Manfred Albrecht ⁴, Florian Kronast ⁵,
Unai Atxitia ³, Clemens von Korff Schmising ² and Wolfgang Kuch ¹

¹*Institut für Experimentalphysik, Freie Universität Berlin, Arnimallee 14, 14195 Berlin, Germany*

²*Max-Born-Institut für Nichtlineare Optik und Kurzzeitspektroskopie, Max-Born-Straße 2A, 12489 Berlin, Germany*

³*Instituto de Ciencia de Materiales de Madrid, CSIC, Cantoblanco, 28049 Madrid, Spain*

⁴*Institute of Physics, University of Augsburg, Universitätsstraße 1, 86135 Augsburg, Germany*

⁵*Helmholtz-Zentrum Berlin für Materialien und Energie, Albert-Einstein-Straße 15, 12489 Berlin, Germany*



(Received 12 June 2025; revised 29 September 2025; accepted 7 October 2025; published 5 November 2025)

The tremendous interest in the technology and underlying physics of all-optical switching of magnetization brings up the question of how fast the switching can occur and how high the frequency of writing the data with ultrafast laser pulses can be. To answer this question, we excited a GdFe ferrimagnetic alloy, the magnetization of which can be reversed by single laser pulses, a phenomenon known as toggle switching, by two pulses with a certain time delay in between. Using photoemission electron microscopy and Kerr microscopy for magnetic domain imaging, we explore the effects of varying fluences of the first and second pulse as well as the time delay between the two pulses. Our results show that when the fluence of the first pulse is adjusted just above the threshold of single-pulse switching, a second pulse with about 60 % of the fluence of the first pulse, arriving only 3 ps later, switches the magnetization back. This reswitching persists up to about 40 ps pulse separation. We interpret the latter as the time required for the sample to cool down and remagnetize after the first pulse. For shorter time delays below about 2 ps, no reswitching occurs. However, the effect of the two pulses adds up, enabling switching for fluences of both pulses below the threshold for single-pulse switching. Atomistic spin dynamics simulations are used to model the experimental data, successfully confirming our results.

DOI: [10.1103/h8j7-4f2z](https://doi.org/10.1103/h8j7-4f2z)

I. INTRODUCTION

Ultrafast all-optical switching (AOS) of magnetization has garnered significant research because of its importance in both fundamental understanding and potential technological advancements [1,2]. It offers a promising solution for developing faster and more energy-efficient magnetic data storage devices. AOS was first observed as helicity-dependent switching in the GdFeCo ferrimagnetic alloy [3], where right and left circularly polarized laser pulses changed the direction of the magnetization in opposite directions without the need for an external magnetic field. Some years later, it was observed that magnetization switching can also be achieved with linearly polarized or unpolarized laser pulses, a process referred to as helicity-independent switching or thermal switching [4,5] and has been termed “toggle switching”. Toggle switching is not limited to GdFeCo alloys but occurs also in synthetic ferrimagnets such as rare-earth/transition metal multilayers [6,7] and in Mn₂Ru_{0.9}Ga Heusler alloy, a rare-earth-free ferrimagnet [8]. In the course of improving the understanding of AOS, the question was raised as to the maximum frequency

at which the magnetization can be optically reswitched. To investigate this, experiments using two single pulses with an adjusted time delay (t_d) between them were conducted. In 2021, Wang and colleagues observed that the Gd₂₇Fe₆₄Co₉ alloy with magnetic compensation temperature of $T_M = 470$ K requires a minimum delay of 300 ps of the second pulse to switch back [9]. They pointed out that this is the minimum time needed for the alloy to cool down to 470 K, the highest temperature at which the sample can switch. The time delay between two pulses should be long enough for the sample to reach this temperature, after which the second pulse can induce the switch back. The researchers suggested that altering the composition of the sample and improving the heat diffusion could potentially increase the switching frequency [9]. In 2022, Steinbach *et al.* examined the idea of optimizing heat diffusion using different substrates, such as amorphous glass, diamond, and silicon, which possess different heat conductivities [10]. Although they emphasized different fluence thresholds for single-pulse toggle switching on each substrate, the GdFe alloy did not reswitch for time delays below 300 ps. They reported a time window between 300–500 ps for reswitching on diamond and silicon substrates. However, they demonstrated that reliable reswitching is achievable in a GdCo alloy with a pulse-to-pulse separation of 7 ps, approaching THz frequency rates for writing and reading data. In this case, the fluence of the second pulse had to be at least 20% higher than that of the first pulse. Double-pulse switching has also

Published by the American Physical Society under the terms of the [Creative Commons Attribution 4.0 International](https://creativecommons.org/licenses/by/4.0/) license. Further distribution of this work must maintain attribution to the author(s) and the published article's title, journal citation, and DOI.

been studied in $\text{Mn}_2\text{Ru}_{0.9}\text{Ga}$ Heusler alloys, where reswitching occurs at 12 ps, faster than in GdFe and GdFeCo. Banerjee *et al.* highlighted that the reswitching frequency is related to the spin-lattice relaxation time and the time needed for magnetic damping [8]. Here, we study double-pulse switching in a GdFe thin-film alloy on a Si substrate using the magnetic imaging techniques photoemission electron microscopy (PEEM) and Kerr microscopy. After determining the threshold for single-pulse switching for an individual laser pulse, we systematically study the sample's response to double-pulse excitation, varying the fluences of both pulses and the time delay between them. The study is divided into two parts: First, we apply double pulses with short time delays of less than or equal to 2 ps and image the magnetic state of the sample using PEEM. Depending on the initial temperature of the sample and the fluences of the two pulses, different response regimes are observed, including switching, no switching, or multidomain formation. In this time-delay range, the sample does not reswitch. Second, for longer time delays, we use Kerr microscopy and observe that if the fluence of the first pulse is just above the threshold for single-pulse switching, a weaker second pulse in a certain fluence window of about 40–60% of the first pulse can reswitch the sample at a time delay as short as 3 ps at room temperature (RT). We compare our experimental results to atomistic spin simulations based on the stochastic Landau-Lifshitz-Gilbert equation and a two-temperature model. The simulations reproduce the experimental observations of suppression of toggle switching of the magnetization by a weaker second pulse with a few ps delay in a certain fluence window and confirm the reswitching of the sublattice magnetizations by the second pulse.

II. EXPERIMENT

The sample has the structure Al (3)/Gd₂₆Fe₇₄ (10)/Pt (5)/substrate (nominal layer thicknesses are given in nm). The Al serves as a capping layer to prevent oxidation. The film was prepared at RT on a 100 nm thick thermally oxidized Si(001) substrate using DC magnetron sputter deposition (chamber base pressure $<10^{-8}$ mbar) from elemental targets utilizing Ar gas at a sputter working pressure of 3.5 μbar . The composition and thickness of the GdFe alloy were determined by Rutherford backscattering spectrometry. The ferrimagnetic GdFe layer has an out-of-plane easy axis of magnetization with 7 mT coercivity at RT. To study the AOS of the sample, we use two microscopic methods, Kerr magneto-optical microscopy and PEEM for acquiring static domain images of the sample after excitation with single or double laser pulses. For PEEM, the setup at the UE49-PGM SPEEM beamline of the BESSY II synchrotron radiation source was used [11], with the photon energy of the circularly polarized x rays set at 707.1 eV at the Fe L_3 edge. A small electromagnet inside the sample holder allows for applying a magnetic field to the sample to saturate the magnetization before applying laser pulses. The images represent pixel-by-pixel differences from the initial saturated state of the sample. The PEEM measurements were performed both at RT and, cooling the sample, at 70 K. The Kerr microscope as described in Ref. [12] was used at RT with an external electromagnet enabling sample saturation.

For exciting the sample, we used linearly p -polarized laser pulses with a wavelength of 800 nm and a pulse length of 100 fs for the optical setup at PEEM, and a wavelength of 1030 nm with a pulse length of 250 fs for the Kerr microscope. Both optical setups include a beam splitter and an optical delay line, allowing us to control the time delay between the two pulses. The two pulses are spatially overlapped on the sample. Since we are using two different setups for imaging, the shape of the laser footprint on the sample and, consequently, the switching area in the sample is different. Both laser profiles follow Gaussian shapes. At the PEEM setup, the laser is focused on the sample at a grazing angle of 16° with respect to the surface and a spot size of about $11 \times 30 \mu\text{m}^2$ (FWHM). In the Kerr microscope setup, the two pump pulses reach the sample at $\pm 76^\circ$ relative to the surface, with a spot size of $63 \times 66 \mu\text{m}^2$ (FWHM). As a result of the different incidence angles, the incident fluence for the switching threshold also varies between the two setups. To avoid any confusion, all fluence values are given as absorbed peak fluence of the GdFe layer, at the center of the laser spot. The absorption of the light in each layer of the sample is calculated and can be found in Fig. S1 within the Supplemental Material [13]. Experimentally, the threshold values of the absorbed fluence determined in that way differ significantly in the two setups, being (at room temperature) 3.4 mJ/cm^2 in the PEEM setup and 0.9 mJ/cm^2 in the Kerr microscope setup. A number of possible reasons can be cited for that: Different actual thresholds for the different pump wavelengths and different temporal pulsewidths, inaccuracies in the determination of the spot sizes, and neglect of interface roughnesses in the calculation of the differential absorption profile.

III. THEORY

We performed atomistic spin dynamics (ASD) computer simulations to model the AOS in the sample. We consider a classical Heisenberg spin Hamiltonian,

$$\mathcal{H} = - \sum_{i \neq j(ij)} J_{ij} \mathbf{s}_i \mathbf{s}_j - \sum_i d_i^z (\mathbf{s}_i^z)^2. \quad (1)$$

Here, $|\mathbf{s}_i| = 1$ represents the normalized classical spin vector at site i . The two sublattices have different and antiparallel atomic magnetic moments μ_{Fe} and μ_{Gd} . We consider both intra- ($J_{\text{Fe-Fe}}, J_{\text{Gd-Gd}} > 0$) and inter-sublattice ($J_{\text{Fe-Gd}} < 0$) exchange coupling parameters. It is assumed that the atomic species of the Gd₂₆Fe₇₄ alloy are randomly distributed within the lattice structure. The dynamics of each atomic spin follows the stochastic Landau-Lifshitz-Gilbert (LLG) equation, which can be found in detail with all the parameters used in Sec. VI of the Supplemental Material [13]. In our simulations, the electron and lattice energy dynamics are modeled using the following two-temperature model:

$$C_c(T_e) \frac{\partial T_e}{\partial t} = G_{ep}(T_{ph} - T_e) + P_1(t) + P_2(t), \quad (2)$$

$$C_{ph} \frac{\partial T_{ph}}{\partial t} = G_{ep}(T_e - T_{ph}) + \frac{T_0 - T_{ph}}{\tau_d}, \quad (3)$$

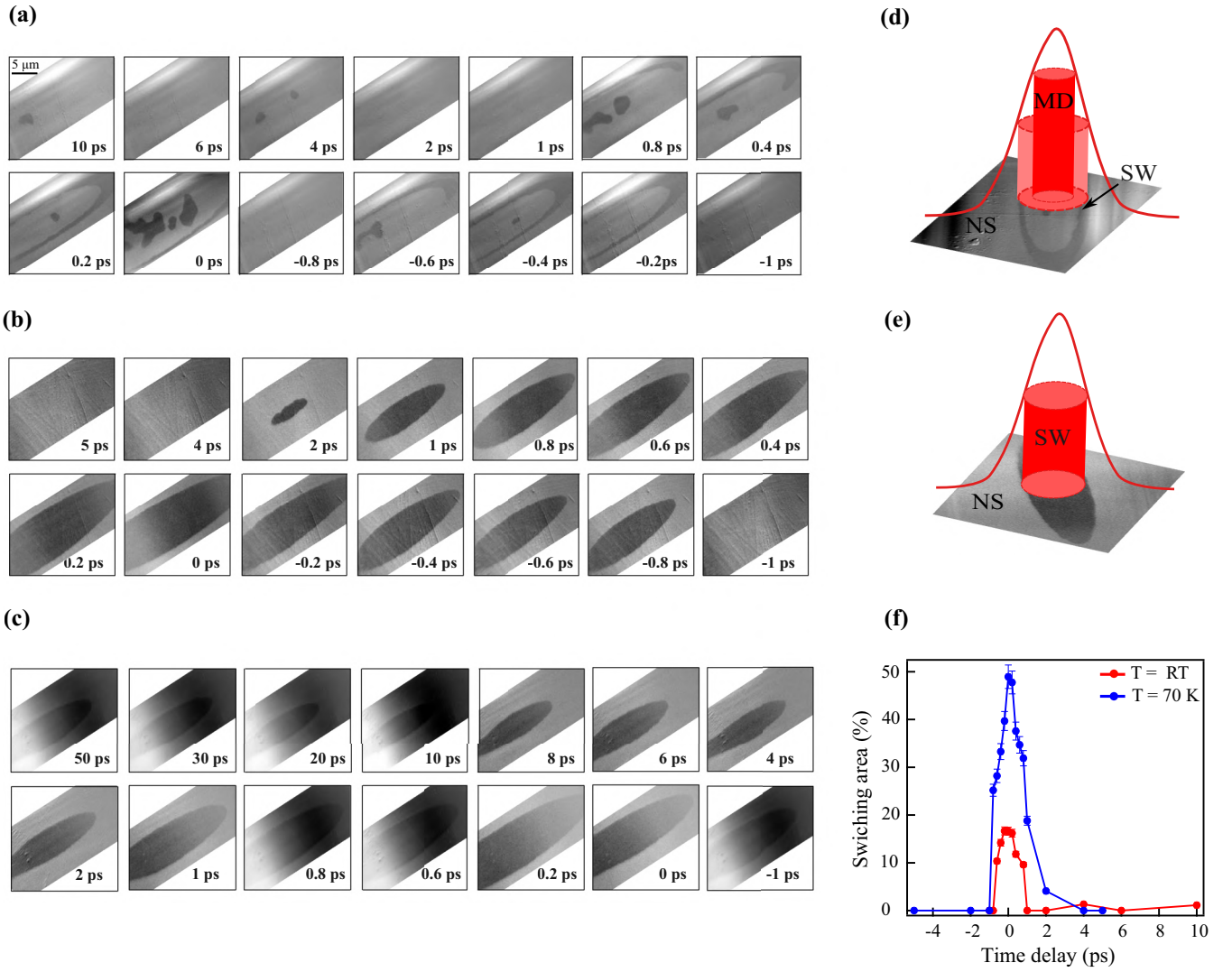


FIG. 1. Static XMCD-PEEM images acquired at the Fe L_3 edge after double-pulse excitation. Each image presents a specific time delay between the two pulses, as written on the bottom right of each image. Dark and light gray contrast corresponds to opposite directions of magnetization. (a) Images measured at room temperature, while the absorbed fluence in the GdFe layer is $F_1 = 2 \text{ mJ/cm}^2$, $F_2 = 2.9 \text{ mJ/cm}^2$. (b) The same experiment performed at 70 K, with absorbed fluence in the GdFe layer $F_1 = 2 \text{ mJ/cm}^2$, $F_2 = 2.9 \text{ mJ/cm}^2$. In both cases, both fluences are below the threshold for magnetic toggle switching, which is $F_{1th} = F_{2th} = 3.4 \text{ mJ/cm}^2$. (c) The same experiment, done at 70 K with absorbed fluence $F_1 = 4.7 \text{ mJ/cm}^2$, $F_2 = 0.7 \text{ mJ/cm}^2$, where the fluence of the first pulse is above the threshold of single-pulse toggle switching, which is $F_{1th} = F_{2th} = 3.8 \text{ mJ/cm}^2$ at 70 K. (d), (e) Sketches of the Gaussian distribution of laser intensity on top of the final magnetic state of the sample after double-pulse excitation show the different regimes of switching at room temperature and 70 K, respectively. (f) The area of the switching after double-pulse excitation for the cases in panels (a) and (b). The field of view in all images is $20 \times 20 \mu\text{m}^2$.

where T_e , T_{ph} , and T_0 represent electron, phonon, and equilibrium ambient temperatures, respectively. Here, $C_e(T_e) = \gamma_e T_e$, with $\gamma_e = 6 \times 10^2 \text{ Jm}^{-3} \text{ K}^{-2}$.

To align the electron and lattice temperature dynamics with those calculated by a two-temperature model considering all layers and the substrate of the sample as well as vertical heat transport across the layers as described in the Supplemental Material of Ref. [14] (see also Sec. VII of the Supplemental Material [13]), we slightly increased the phonon heat capacity to $C_{ph} = 2.5 \times 10^6 \text{ Jm}^{-3} \text{ K}^{-1}$ and the electron-phonon coupling to $G_{ep} = 7.0 \times 10^{17} \text{ W m}^{-3} \text{ K}^{-1}$. The last term in Eq. (3) corresponds to the phenomenological cooling term that we included in our model. The relaxation time (τ_d) was

adjusted to achieve good agreement with the two-temperature model of the full layered stack including vertical heat flow across the sample layers. For the laser power functions, $P_1(t)$ and $P_2(t)$ in Eq. (2), we assumed Gaussian shapes following Ref. [14], both in Eq. (2) and in the full two-temperature model.

IV. RESULTS

Figure 1 shows the switching behavior recorded by PEEM at two different sample temperatures, RT and 70 K. The two different contrasts in the images indicate opposite directions of the magnetization; dark contrast represents domains of

switched magnetization. The straight bright and dark stripes seen in all images of Fig. 1(a) are artifacts caused by the distribution of x-ray intensity across the field of view. In Fig. 1(a), the sample is at room temperature, and the fluence of both pulses is below the threshold of single-pulse switching, meaning that each pulse alone is insufficient to switch the sample. However, when both laser pulses excite the sample, switched areas are observed for time delays between them of less than 1 ps. These switched regions appear as irregular dark domains in the center of the laser spot, as well as elliptical patterns following the footprint of the laser spot on the sample. We can thus distinguish three regions in the sample based on the local fluence of the laser. The first region, located at the center of the laser spot where the fluence is highest, presents a random multidomain (MD) pattern, probably as a consequence of a complete demagnetization [15]. The second region, consisting of dark ellipses, corresponds to intermediate fluences located in the gradient of the spatial laser profile and closely follows the shape of the laser spot. In this area, the sample undergoes deterministic toggle switching (SW). The third region, located at the lowest fluence, outside the ellipses, shows no switching (NS). The corresponding boundary fluences between these regions vary depending on the time delay between the pulses. For example, the inner line of constant fluence between MD and SW areas at $t_d = 0.2$ ps is approximately at $F_1 = 0.85F_{1,\text{Max}}$, $F_2 = 0.83F_{2,\text{Max}}$, where F_{Max} represents the peak fluence, while at $t_d = 0.8$ ps, these fluences decrease to approximately $F_1 = 0.70F_{1,\text{Max}}$ and $F_2 = 0.64F_{2,\text{Max}}$. Small deviations from a perfect spatial overlap of the two pulses could be the reason why in some of the panels of Fig. 1(a) the dark areas of the SW regions are wider on one side of the ellipses than on the other.

Figure 1(b) depicts the switching behavior of the sample at short time delays at 70 K, which is below the magnetic compensation temperature T_M and the angular momentum compensation temperature T_A . As with the RT case, the fluences of both pulses are below the threshold for single-pulse switching. Similar to the behavior at RT, a switched area appears for time delays shorter than 2 ps. However, at 70 K, the sample only shows two distinct regions, the SW region at higher fluences and the NS region at lower fluences. No multidomain formation is observed at this temperature. Compared to Fig. 1(a), the presence of a SW region at delays of 2, 1, and -0.8 ps, together with a larger size of the switched area at some delays, could be an indication for a lower threshold for double-pulse switching at the lower base temperature. The absence of the MD regime in Fig. 1(b) suggests that the mobility of domain walls is likely higher at RT than at 70 K, lowering the threshold for domain formation and facilitating the appearance of multidomain patterns after transient demagnetization of the sample at RT. Figure 1(c) shows the results for the case where the fluence of the first pulse is above the threshold for single-pulse toggle switching while the second pulse remains below this threshold. The temperature is maintained at 70 K, as in Fig. 1(b). Now a switched area is observed for all time delays caused by the first pulse alone. The switched area expands to lower local fluences for delays shorter than 2 ps, to regions of the sample that are not switched at larger temporal separations between the two pulses. This behavior is thus consistent with that observed in Fig. 1(b).

The effect of the second pulse obviously enhances the effect of the first pulse at these very short time delays, regardless of whether both pulses are below the threshold or one is above the threshold. Figures 1(d) and 1(e) illustrate the laser profile at the two temperatures to help visualize it. The area of the switching at RT and 70 K for the cases in which both pulses are below threshold of the single-pulse switching is plotted in Fig. 1(f), where it is shown that the switched area decreases rapidly at higher time delays.

In none of these cases does the sample reswitch. To investigate this further, we study the double-pulse switching behavior of the sample using Kerr microscopy at RT, examining different fluences for longer time delays. Figure 2 depicts the static state of the sample following double-pulse excitation of the saturated state that appears as a light-gray contrast for various fluence combinations and time delays. The three panels correspond to three different fluences of the first pulse F_1 , as indicated on the left. The three images on the left show the result of only the first pulse. $F_1 = 0.78$ mJ/cm² is below the threshold for single-pulse toggle switching, while 0.91 and 1.04 mJ/cm² are just above and well above this threshold, respectively. The bottom axis indicates the time delay between the two pulses, while the fluence of the second pulse is given on the right axes. The behavior of single-pulse excitation at different fluences can be found in Fig. S2 within the Supplemental Material [13]. Both laser pulses are *p*-polarized and spatially overlap on the sample; therefore, at time zero, where both pulses temporally overlap, an interference pattern appears [16]. In the first panel, with $F_1 = 0.78$ mJ/cm² and $t_d = 1$ ps, we observe only SW region for $F_2 = 0.13$ mJ/cm², indicating that, although the sample does not switch with the first pulse alone, adding a second pulse with $F_2 = 0.13$ mJ/cm² is enough to switch the sample as long as the time delay between the two pulses is 1 ps or less, similar to the findings presented before. Increasing F_2 to 0.26 mJ/cm² allows switching to be observed up to a delay time of 3 ps, albeit with a decreasing size of the switched area as the delay increases. From $F_2 = 0.39$ mJ/cm², a small region of light-gray contrast appears in the center of the switched area, where the fluence is highest, and this region increases further with higher F_2 values. This trend is also observed for the other F_1 fluences in Fig. 2 at 1 and 2 ps when the sum of F_1 and F_2 exceeds approximately 1.17 mJ/cm². Increasing the time delay between the two pulses at $F_1 = 0.78$ mJ/cm² brings the sample to the NS state, which means that for this relatively low F_1 , the effect of the first pulse has already relaxed too much to allow the sample being switched by the second pulse. The probability of finding the sample in the nonswitched state after the second pulse follows a nonmonotonic trend. At $F_2 = 0.52$ mJ/cm², already at 3 ps the sample is found predominantly in the NS state (see also Fig. S10 of the Supplemental Material [13] for repeated switching experiments at $F_1 = 0.78$ mJ/cm² [13]), while at both, lower and higher F_2 , switched areas are observed at longer time delays.

A nonmonotonic behavior is also observed in the center panel, for $F_1 = 0.91$ mJ/cm², where F_1 is high enough to switch the sample with the first pulse alone. Here, for $F_2 = 0.39$ mJ/cm², the switched area is largely suppressed for delays from 4 to 20 ps, and at $F_2 = 0.52$ mJ/cm², this extends over an even broader delay range. In the bottom

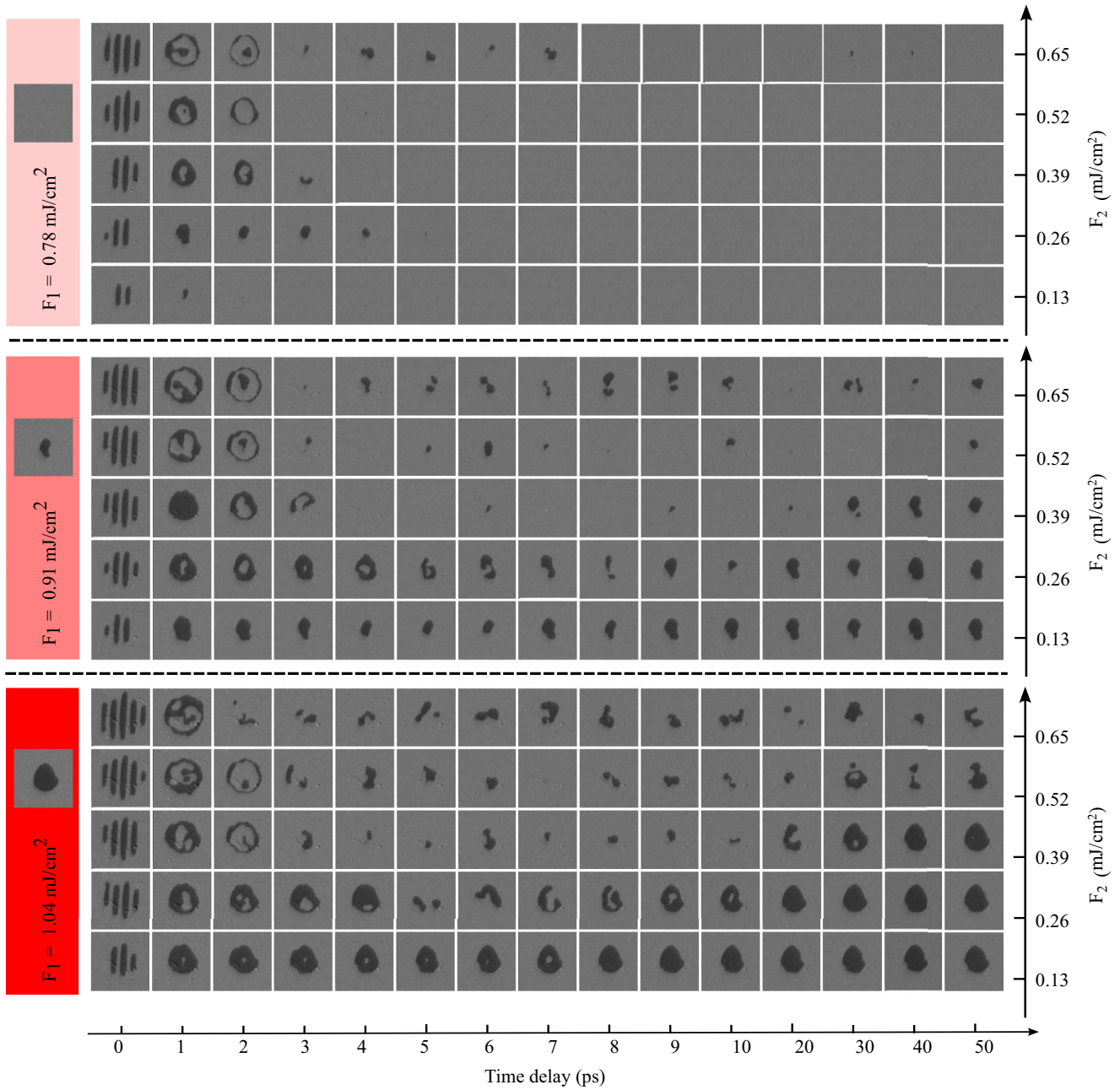


FIG. 2. Kerr microscopy images after excitation with two pulses at room temperature. Dark and light gray contrasts correspond to opposite directions of magnetization. The bottom axis shows the time delay between the two pulses. The left column shows the absorbed fluence of the first pulse. It also includes an image of single-pulse switching at these fluences. The right axes show the absorbed fluence of the second pulse. The field of view is $50 \times 50 \mu\text{m}^2$.

panel, for $F_1 = 1.04 \text{ mJ/cm}^2$, a shrinking of the switched area is evident for time delays between 3 and about 10 ps at $F_2 = 0.39$ and 0.52 mJ/cm^2 . This shrinking indicates that, at fluences slightly below the maximum fluence, corresponding to the center in the Gaussian footprint of the laser pulses, no switching occurs. This suggests that reswitching of the sample by the second pulse occurs within a specific fluence range of the second pulse, depending on the fluence of the first pulse. However, when the fluence of the second pulse is increased excessively, for example to 0.65 mJ/cm^2 , the sample probably overheats, resulting in the formation of an MD pattern.

To study the occurrence of the reswitching more precisely, we focus on $F_1 = 0.91 \text{ mJ/cm}^2$ while changing F_2 in smaller steps. The results are shown in Fig. 3, where the left axis displays the fluence of the second pulse, ranging from 0.13 to 0.52 mJ/cm^2 , and the bottom axis shows the time delay between the two pulses. As the fluence of the second pulse is increased at $t_d = 4 \text{ ps}$, an MD region first develops at the center of the pulse spots, and then, at $F_2 = 0.36 \text{ mJ/cm}^2$, reswitching begins as indicated by a yellow frame. At $t_d = 8 \text{ ps}$, reswitching occurs at a lower fluence of $F_2 = 0.31 \text{ mJ/cm}^2$, which is the minimum fluence of the second pulse required to completely reswitch the sample at this F_1 .

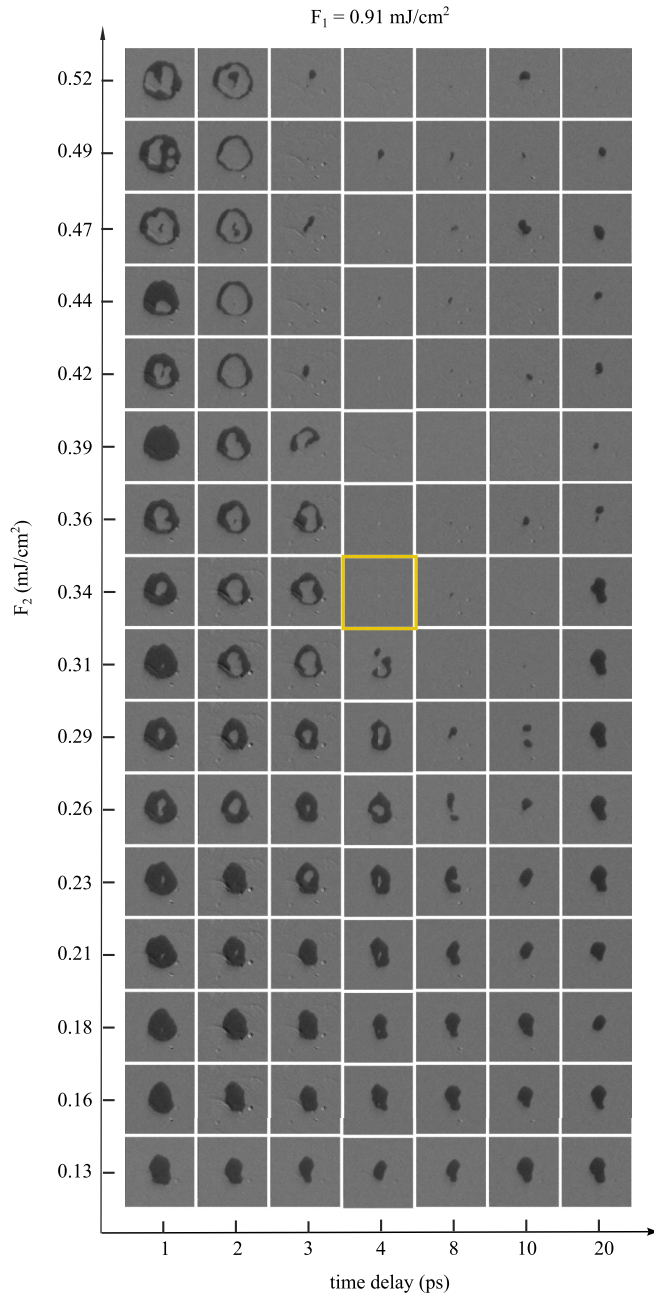


FIG. 3. The magnetic state of the sample after double-pulse excitation when the absorbed fluence of the first pulse is 0.91 mJ/cm^2 , just above the threshold for all-optical toggle switching. The left axis shows the absorbed fluence of the second pulse increasing in small steps below the threshold for single-pulse switching. The bottom axis shows the time delay. The images are recorded at room temperature and the field of view is $50 \times 50 \mu\text{m}^2$.

V. DISCUSSION

To better understand the mechanism behind double-pulse switching and reswitching, we carried out atomistic spin dynamic (ASD) simulations [17–20]. The reswitching probability from these simulations is shown in Fig. 4 for a fixed fluence F_1 of the first pulse. Bright to dark colors indicate the probability of reswitching the magnetization by the second pulse, obtained from 15 individual simulations, each

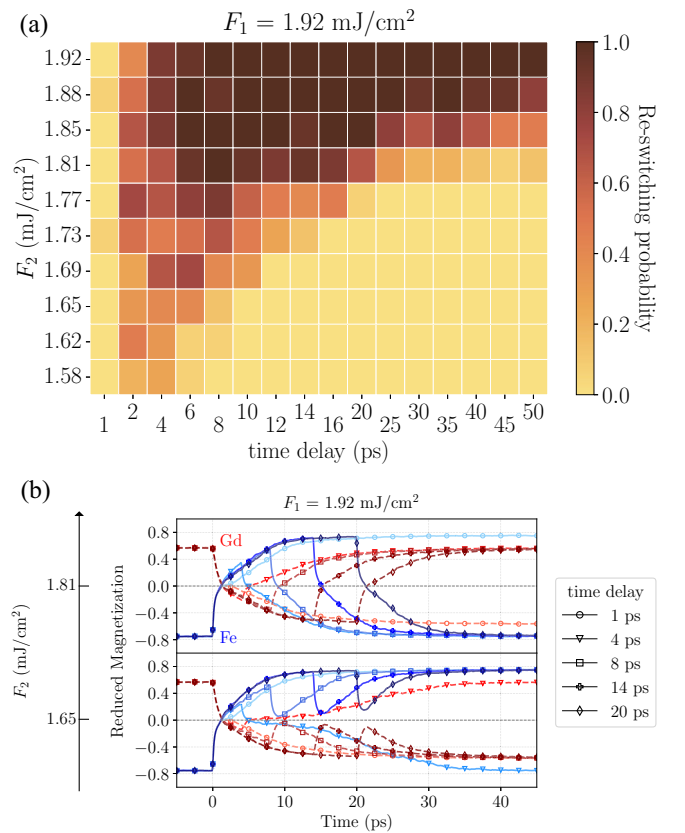


FIG. 4. (a) The calculated probability of reswitching the magnetization after double-pulse excitation. The fluence of the first pulse is constant and corresponds to the threshold for single-pulse switching, which is 1.92 mJ/cm^2 . Bright and dark colors in panel (a) correspond to no reswitching and reswitching, respectively, while intermediate shades represent the probability of reswitching, as shown in the legend. (b) The magnetization of each sublattice, normalized to one for $T = 0$, as a function of time for two selected fluences of the second pulse, $F_2 = 1.81$ and 1.65 mJ/cm^2 , as shown on the left axis. The Fe magnetization is shown in blue colors and the one of Gd in red. The time delay between the two pulses is indicated by different symbols in the legend.

corresponding to the outcome of an individual simulation using the LLG equation with the Hamiltonian given in Eq. (1). The fluence of the first pulse F_1 is set just above the single-pulse switching threshold. In the simulations, this threshold is 1.92 mJ/cm^2 , which is roughly twice the experimental value. While simulations of single pulses with 1.92 mJ/cm^2 always result in switching, the outcome of individual simulations with combinations of F_1 , F_2 , and t_d close to the switching threshold exhibits significant variability because of the nature of the stochastic Landau-Lifshitz-Gilbert (LLG) equation. The color gradient between dark and bright in the plot indicates the reswitching probability from 15 individual simulations. In the figure, the fluence of the second pulse increases along the vertical axis while the delay time progresses along the horizontal axis. This allows for comparison with Figs. 2 or 3 from the experiment, where one has to keep in mind that the simulations do not include dipolar interactions and thus will not reproduce multidomain formation. The simulations qualitatively reproduce the same behavior observed experimentally. At $t_d = 1 \text{ ps}$,

the sample switches, but beginning at $t_d = 2$ or 4 ps, reswitching occurs for F_2 values exceeding a certain threshold, around 1.77 mJ/cm^2 . This consistency between simulations and experiments helps confirm the key role of the time delay and fluence in controlling the switching dynamics, with stochastic effects playing a significant role in determining the exact behavior at specific parameter combinations. The reswitching dynamics become increasingly complex as the time delay increases. The maximum delay time after which the presence of the second pulse can hinder the sample from being switched increases with increasing F_2 , as in the experiment. Figure 4(b) shows the simulated time traces of the Gd and Fe sublattice magnetizations for ten distinct combinations of F_2 and t_d from panel Fig. 4(a). After the first laser pulse excites the sample, its energy raises the electron temperature T_e , which then dissipates to the phonon system via electron-phonon coupling, establishing an equilibrium between the electron and phonon temperatures within 2 ps. Previous theoretical work has shown that a certain amount of reversed magnetization of both sublattices, about 20%, at the time of the second pulse is necessary to induce reswitching [21]. From the experiment conducted by Radu *et al.* [4] it is known that for single-pulse switching the Fe sublattice in GdFeCo demagnetizes within 300 fs, while the Gd sublattice takes longer, approximately 1.5 ps. Another work checked the XMCD as well as the calculation for GdFeCo alloy and reported that Fe demagnetizes in 0.4 ps and Gd in 1.2 ps [22].

Therefore, if the second pulse is applied at $t_d = 1$ ps before the electron and phonon systems reach equilibrium, the sublattices are still in the course of demagnetization [as shown in Fig. 4(b)]. At this stage, the magnetization of both sublattices is close to zero, still demagnetizing and not yet reversed. The second laser pulse adds additional energy into the system, pushing the sublattice magnetization further toward zero and thereby contributing to the demagnetization process, which ultimately results in a single switching event. In contrast, for $t_d = 4$ ps, both sublattice magnetizations have already crossed zero, making it possible for the second pulse to reverse the magnetization and induce reswitching, as shown in Fig. 4(b). The simulated time trace for 4 ps time delay clearly shows that the reswitching trajectory after the second pulse differs from that of a single switching event, which is plausible, since it starts from a higher temperature. The longer the delay between the two pulses, the more the magnetization of the sublattices stabilizes in opposite directions as the sample cools further. The more the sample has cooled, the higher fluences F_2 are necessary to initiate the reswitching. This is in agreement with the experimental observation that when the first pulse is set at the switching threshold, increasing the fluence of the second pulse results in reswitching being observed over a larger time-delay window. In the examples selected for Fig. 4(b), both at $t_d = 8$ ps and $t_d = 14$ ps, a second pulse of 1.81 mJ/cm^2 is able to reswitch the sample, while 1.65 mJ/cm^2 is insufficient for reswitching. According to the experimental result of Ref. [4], at 3 ps the sublattice magnetizations have already crossed zero and begun to re-magnetize in the opposite direction. Therefore, for time delays longer than 3 ps, the magnetization of both sublattices has sufficient time to recover after the first switching, and if the second pulse carries enough energy, it can switch both sublattices

again. This has also been recently found in calculations of double-pulse switching in GdFe [23].

The effect of the second pulse also depends on the amount of sublattice magnetization reversed by the first pulse. Shortly after crossing zero, when only a small amount of reversed sublattice magnetization is present, a stronger second pulse is needed to pull the magnetizations back across zero (see, for example, Fig. S11 within the Supplemental Material [13] at 4 ps time delay). This is observed in Fig. 3, where the minimum time required for reswitching increases when decreasing the fluence of the second pulse down to 0.31 mJ/cm^2 , leading to a narrower delay-time window for reswitching at lower F_2 . The threshold fluence for the second pulse for reswitching consequently decreases with increasing time delay from 4 to about 10 ps, as seen in both the experiment and the simulations. The reason for this could be that at the higher temperatures present at shorter delays, the demagnetization dynamics of the Gd and Fe sublattices become more similar [24], making it harder for the second pulse to toggle the magnetization.

At even longer time delays, the sample only toggle-switches, and the second pulse does not have any effect on reswitching or demagnetizing the sample as long as its fluence is below the single-pulse switching threshold. This leads to an increase of the threshold fluence of the second pulse for reswitching with increasing time delay at delays greater than about 10 ps. This is observed in both the experimental data and the simulation results. It is also discussed in the theory work of Ref. [25] as a possible scenario for double-pulse switching. In this case, the first pulse switches the sample, and by the time the second pulse adds energy, the sample has already cooled down, making it insufficient for either reswitching or demagnetizing.

A study of Fe/Gd bilayers highlights the ultrafast demagnetization dynamics of both sublattices, with Fe demagnetizing in 0.7 ps and Gd in 3.4 ps at room temperature (RT) [26]. The authors of that study attribute the demagnetization to magnons and argue that the thickness of the individual layers plays a crucial role, as magnons must traverse the layers to transfer magnetic moments to layers farther from the interface [26], wherein in GdFeCo alloys, Fe and Gd atoms are separated by just a few Å; the transfer of magnetic moments is faster, leading to even shorter demagnetization times. Steinbach *et al.* reported reswitching in Gd₂₄Fe₇₆ (20 nm) on a Si substrate, with a calculated T_c of 515 K occurring approximately at 500 ps [10], while for GdCo alloys, with a calculated T_c of 570 K, reswitching was observed at 7 ps for fluences of the second pulse >1.2 times the one of the first pulse. The different times were discussed as a result of the higher exchange interactions within the transition metal sublattice when replacing Fe with Co in the alloy, leading to faster recovery times and reswitching of GdCo [10,17]. In the present study, in contrast, for 10 nm Gd₂₆Fe₇₄ on a Si substrate with a calculated T_c of 540 K, we observe reswitching at 4 ps if the fluence of the first pulse is tuned to just above the threshold of single-pulse switching and the fluence of the second pulse is on the one hand sufficiently high to reverse the sublattice magnetizations, but on the other hand also sufficiently low to not lead to full demagnetization and MD formation. This fast reswitching regime may have been

overlooked in previous investigations, or may not be present in different samples with different film thicknesses and alloy compositions. The T_c of our sample is similar to that of GdCo of Ref. [10], which may explain the fast recovery towards the reversed magnetization after the first pulse in our experiments. Additionally, T_M is likely different between the different samples. It has been shown theoretically that the minimum pulse separation for reswitching depends strongly on the slope of the net magnetization with temperature at the measurement temperature and thus on the compensation temperature, at which this slope becomes zero [21]. A higher compensation temperature relative to the measurement temperature allows for faster double switching. Since T_M varies strongly with the alloy composition, this may also explain the different behavior observed in the different studies.

Figure 5(a) displays the simulated switching probability when the first pulse is set below the threshold of single-pulse switching. The vertical axis represents the fluence of the second pulse and the horizontal axis the delay between the two pulses. This can be compared to the experimental results in the first row of Fig. 2, for $F_1 = 0.78 \text{ mJ/cm}^2$. The simulations show that, for a time delay of 1 ps, the energy from both pulses adds up to switch the sample magnetization, as seen in the experiment. This is also partly the case at $t_d = 2 \text{ ps}$, with a higher probability for larger second-pulse fluences. The dynamics of the sublattice magnetizations are presented in Fig. 5(b) for four selected values of F_2 and five representative delay times. For $t_d = 1 \text{ ps}$, the second pulse arrives while the sample is still demagnetizing from the first pulse, adding energy and pushing the sublattice magnetizations across zero, like one stronger pulse. For longer time delays, whether switching occurs or not depends on the fluence of the second pulse. Generally, the higher F_2 , the greater the switching probability at longer t_d . This depends on how much the sublattice magnetizations have recovered after the first pulse. More recovery requires a higher fluence of the second pulse to induce switching. In the simulation, at $F_1 = 1.78 \text{ mJ/cm}^2$, the sample switches more reliably at longer time delays (10 or 14 ps) than at shorter ones (2 or 4 ps). Inspecting Fig. 5(b), this can be understood as follows: The demagnetizing effect of the second pulse at a fixed F_2 depends on the transient temperature of the sample, and therefore the sublattice magnetizations when the second pulse arrives. For example, in the simulation shown in the top panel of Fig. 5(b), both pulses have the same fluence. At 14 ps after the first pulse, the simulated sublattice magnetizations have nearly fully recovered, meaning the second pulse affects the sublattice magnetization in a manner similar to the first, potentially leading to switching. However, if the second pulse arrives while the sublattice magnetizations are still reduced, for example, at 4 ps, the second pulse's effect on the sublattice magnetizations is diminished, which may result in a situation where switching is less likely at shorter delay times than at longer ones, as observed in the simulations for $F_2 = 1.74 \text{ mJ/cm}^2$ at 2 and 4 ps or at $F_2 = 1.78 \text{ mJ/cm}^2$ and $t_d = 2, 4, \text{ and } 6 \text{ ps}$. In the experiment, there is only one image that shows this effect, namely in Fig. 2 for $F_1 = 0.78 \text{ mJ/cm}^2$, $F_2 = 0.65 \text{ mJ/cm}^2$, and $t_d = 3 \text{ ps}$. Since this happens only in one image, it is, however, not clear whether this effect is really observed or simply caused by statistical variation. However, the experiment was repeated several times, and the same effect

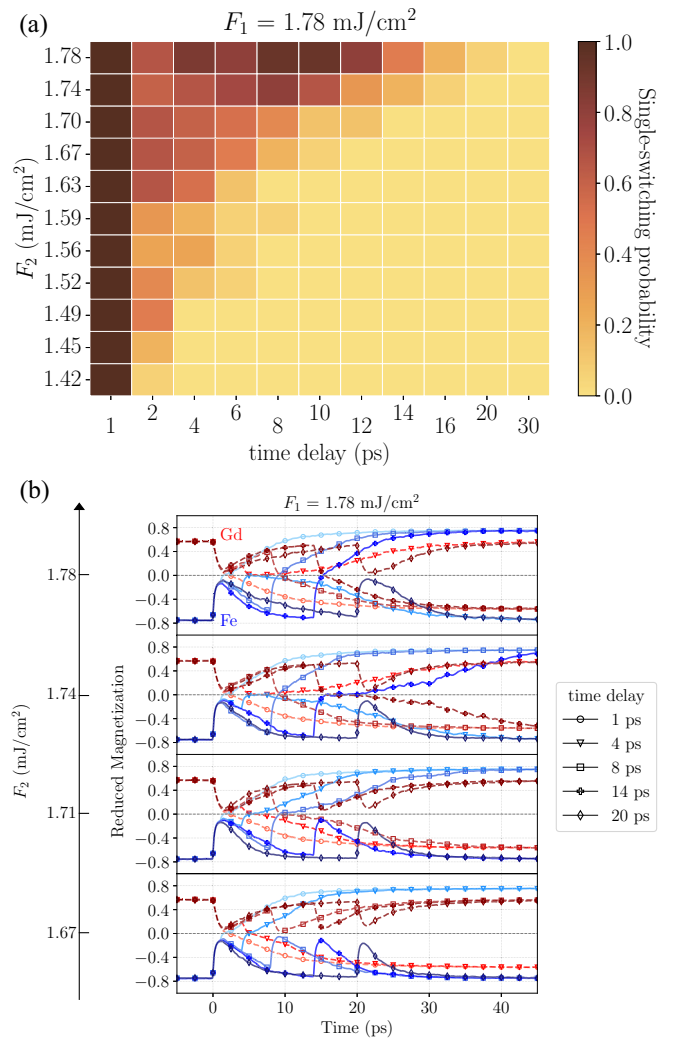


FIG. 5. (a) The probability for switching as a function of the fluence of the second pulse for different time delays. The fluence of the first pulse is constant at $F_1 = 1.78 \text{ mJ/cm}^2$, which is below the threshold of single-pulse switching. Dark and bright colors correspond to switching and no switching, respectively. (b) The magnetization of each sublattice, normalized to one for $T = 0$, as a function of time for four selected fluences of the second pulse, $F_2 = 1.78, 1.74, 1.71 \text{ and } 1.67 \text{ mJ/cm}^2$. The Fe magnetization is shown in blue and the one of Gd in red. The time delay between the two pulses is indicated by different symbols in the legend.

was observed in some of the cases, as shown in Fig. S10 within the Supplemental Material [13].

The absence of switching observed experimentally in the top panel of Fig. 2 for $F_2 = 0.39 \text{ mJ/cm}^2$ and 0.52 mJ/cm^2 as the absence of switched area for $t_d \geq 4$ or 3 ps , respectively, could correspond to the reduced switching probability seen in the simulation at $F_2 = 1.74 \text{ mJ/cm}^2$ and 1.78 mJ/cm^2 with time delays of 2 and 4 ps. However, in the experiment, at these time delays and fluences, significant multidomain formation already occurs. Since magnetostatic effects and domain formation are not included in our simulations, the suppression of switching seen at $F_2 = 0.39 \text{ mJ/cm}^2$ and 0.52 mJ/cm^2 in the experiment may not be fully captured by the simulations.

VI. SUMMARY AND CONCLUSIONS

In conclusion, we have studied the double-pulse switching of the GdFe alloy using PEEM and Kerr microscopy to understand the effect of the different fluences on the reswitching of the magnetization. By comparing the results to atomistic spin dynamics simulations, we were able to pin down the mechanisms and requirements for all-optical switching by two pulses and for reswitching by a second pulse. We found that the shortest time between the two pulses at which reswitching of the sample is observed is 4 ps, corresponding to 250 GHz. This is achieved when the fluence of the first pulse is just above the threshold for single-pulse switching and the second pulse has a fluence of about 0.4–0.7 times that of the first pulse. Reswitching is observed within a certain range of time delays, typically between 4 and 40 ps, which depends on the fluence of the second pulse and increases with higher second-pulse fluences. At these times after the first pulse, the electron and lattice temperature have already equilibrated and the magnetization of each sublattice has moved sufficiently away from zero. However, at shorter temporal distances between the two pulses, when the electron temperature has not yet equilibrated with the lattice temperature, the effect of the two pulses adds up, leading to switching or multi-domain formation, and thus no back-switching occurs. Therefore, to achieve reswitching shortly after a switching event, a fast equilibration of electron and lattice temperatures and efficient heat dissipation to the substrate are required. An essential ingredient for fast reswitching is to carefully select the fluences of the two pulses, with the fluence of the first pulse

slightly above the threshold for all-optical toggle switching and the fluence of the second pulse high enough to trigger another toggle switching event from the not-yet recovered reversed magnetization, but not too high to fully demagnetize the sample. It remains to be seen whether further enhancing the latter by the choice of the substrate material [15] and by fine-tuning the compensation temperature via the GdFe composition could lead to even faster reswitching.

ACKNOWLEDGMENTS

This work was supported by the Deutsche Forschungsgemeinschaft via the CRC/TRR 227 “Ultrafast Spin Dynamics”, Project ID: 328545488, projects A02 and A07. We thank the Helmholtz-Zentrum Berlin for the allocation of synchrotron radiation beamtime. U.A. gratefully acknowledges support by Grants No. PID2021-122980OB-C55, No. PID2024-157112OB-C52 and No. CNS2023-144681 funded by MCIN/AEI/10.13039/501100011033 and by ERDF A way of making Europe and ESF Investing in your future. U.A., J.M.L., and C.v.K.S. acknowledge support from Project ilink23081 from Convocatoria i-LINK 2023 CSIC. J.M.L. acknowledges the award of a Ph.D. Grant from Comunidad de Madrid (PIPF-2023/TEC-29997).

DATA AVAILABILITY

The data that support the findings of this article are openly available [27].

-
- [1] A. V. Kimel, A. M. Kalashnikova, A. Pogrebna, and A. K. Zvezdin, Fundamentals and perspectives of ultrafast photoferroic recording, *Phys. Rep.* **852**, 1 (2020).
- [2] A. Kirilyuk, A. V. Kimel, and T. Rasing, Ultrafast optical manipulation of magnetic order, *Rev. Mod. Phys.* **82**, 2731 (2010).
- [3] C. D. Stanciu, F. Hansteen, A. V. Kimel, A. Kirilyuk, A. Tsukamoto, A. Itoh, and T. Rasing, All-optical magnetic recording with circularly polarized light, *Phys. Rev. Lett.* **99**, 047601 (2007).
- [4] I. Radu, K. Vahaplar, C. Stamm, T. Kachel, N. Pontius, H. A. Dürr, T. A. Ostler, J. Barker, R. F. L. Evans, R. W. Chantrell *et al.*, Transient ferromagnetic-like state mediating ultrafast reversal of antiferromagnetically coupled spins, *Nature (London)* **472**, 205 (2011).
- [5] T. Ostler, J. Barker, R. Evans, R. Chantrell, U. Atxitia, O. Chubykalo-Fesenko, S. El Moussaoui, L. Le Guyader, E. Mengotti, L. Heyderman *et al.*, Ultrafast heating as a sufficient stimulus for magnetization reversal in a ferrimagnet, *Nat. Commun.* **3**, 666 (2012).
- [6] P. Li, T. J. Kools, B. Koopmans, and R. Lavrijsen, Ultrafast racetrack based on compensated Co/Gd-based synthetic ferrimagnet with all-optical switching, *Adv. Electron. Mater.* **9**, 2200613 (2023).
- [7] J. Hintermayr, P. Li, R. Rosenkamp, Y. L. W. van Hees, J. Igarashi, S. Mangin, R. Lavrijsen, G. Malinowski, and B. Koopmans, Ultrafast single-pulse all-optical switching in synthetic ferrimagnetic Tb/Co/Gd multilayers, *Appl. Phys. Lett.* **123**, 072406 (2023).
- [8] C. Banerjee, N. Teichert, K. E. Siewierska, Z. Gercsi, G. Y. P. Atcheson, P. Stamenov, K. Rode, J. M. D. Coey, and J. Besbas, Single pulse all-optical toggle switching of magnetization without gadolinium in the ferrimagnet Mn_2Ru_xGa , *Nat. Commun.* **11**, 4444 (2020).
- [9] S. Wang, C. Wei, Y. Feng, H. Cao, W. Li, Y. Cao, B. Guan, A. Tsukamoto, A. Kirilyuk, A. V. Kimel, and X. Li, Dual-shot dynamics and ultimate frequency of all-optical magnetic recording on GdFeCo, *Light Sci. Appl.* **10**, 8 (2021).
- [10] F. Steinbach, N. Stetzuhn, D. Engel, U. Atxitia, C. von Korff Schmising, and S. Eisebitt, Accelerating double pulse all-optical write/erase cycles in metallic ferrimagnets, *Appl. Phys. Lett.* **120**, 112406 (2022).
- [11] F. Kronast and S. Valencia Molina, SPEEM: The photoemission microscope at the dedicated microfocus PGM beamline UE49-PGMa at BESSY II, *JLSRF* **2**, A90 (2016).
- [12] F. Steinbach, D. Schick, C. Von Korff Schmising, K. Yao, M. Borchert, W. D. Engel, and S. Eisebitt, Wide-field magneto-optical microscope to access quantitative magnetization dynamics with femtosecond temporal and sub-micrometer spatial resolution, *J. Appl. Phys.* **130**, 083905 (2021).
- [13] See Supplemental Material at <http://link.aps.org/supplemental/10.1103/h8j7-4f2z> for additional details, which includes Refs. [14,20,28–33].

- [14] Y. A. Shokr, O. Sandig, M. Erkovan, B. Zhang, M. Bernien, A. A. Ünal, F. Kronast, U. Parlak, J. Vogel, and W. Kuch, Steering of magnetic domain walls by single ultrashort laser pulses, *Phys. Rev. B* **99**, 214404 (2019).
- [15] M. Verges, W. Zhang, Q. Remy, Y. Le-Guen, J. Gorchon, G. Malinowski, S. Mangin, M. Hehn, and J. Hohlfield, Extending the scope and understanding of all-optical magnetization switching in Gd-based alloys by controlling the underlying temperature transients, *Phys. Rev. Appl.* **21**, 044003 (2024).
- [16] No such interference pattern was observed in the PEEM experiments since the two pump pulses arrived at virtually the same angle to the sample.
- [17] F. Jakobs and U. Atxitia, Universal criteria for single femtosecond pulse ultrafast magnetization switching in ferrimagnets, *Phys. Rev. Lett.* **129**, 037203 (2022).
- [18] F. Jakobs and U. Atxitia, Bridging atomistic spin dynamics methods and phenomenological models of single-pulse ultrafast switching in ferrimagnets, *Phys. Rev. B* **106**, 134414 (2022).
- [19] F. Jakobs and U. Atxitia, Exchange-enhancement of the ultrafast magnetic order dynamics in antiferromagnets, [arXiv:2206.05783](https://arxiv.org/abs/2206.05783).
- [20] F. Jakobs, T. A. Ostler, C.-H. Lambert, Y. Yang, S. Salahuddin, R. B. Wilson, J. Gorchon, J. Bokor, and U. Atxitia, Unifying femtosecond and picosecond single-pulse magnetic switching in Gd-Fe-Co, *Phys. Rev. B* **103**, 104422 (2021).
- [21] U. Atxitia and T. A. Ostler, Ultrafast double magnetization switching in GdFeCo with two picosecond-delayed femtosecond pump pulses, *Appl. Phys. Lett.* **113**, 062402 (2018).
- [22] I. Radu, C. Stamm, A. Eschenlohr, F. Radu, R. Abrudan, K. Vahaplar, T. Kachel, N. Pontius, R. Mitzner, K. Holldack *et al.*, Ultrafast and distinct spin dynamics in magnetic alloys, *SPIN* **05**, 1550004 (2015).
- [23] D. Liu, J. Weng, X. Song, W. Cai, S. Tan, and C. Xu, Ultrafast write-read event in helicity-independent all-optical switching of GdFeCo, *J. Magn. Magn. Mater.* **592**, 171824 (2024).
- [24] U. Atxitia, J. Barker, R. W. Chantrell, and O. Chubykalo-Fesenko, Controlling the polarity of the transient ferromagneticlike state in ferrimagnets, *Phys. Rev. B* **89**, 224421 (2014).
- [25] D. Liu, C. Jiang, N. Wang, and C. Xu, Minimum separation between two pump pulses for ultrafast double magnetization switching in GdFeCo, *Appl. Phys. Lett.* **123**, 162401 (2023).
- [26] D. Lawrenz, Ultraschnelle Magnetisierungsdynamik Ferromagnetischer Schichtsysteme, Ph.D. thesis, Freie Universität Berlin, 2024.
- [27] R. Hosseinifar, F. Steinbach, I. Kumberg, J. M. Lendínez, S. Thakur, S. Hadjadj, J. Gördes, C. S. Awsaf, M. Fix, M. Albrecht, F. Kronast, U. Atxitia, C. von Korff Schmising, and W. Kuch, Zenodo (2025), <https://doi.org/10.5281/zenodo.17095652>.
- [28] K. Ohta and H. Ishida, Matrix formalism for calculation of electric field intensity of light in stratified multilayered films, *Appl. Opt.* **29**, 1952 (1990).
- [29] R. Chimata, L. Isaeva, K. Kádas, A. Bergman, B. Sanyal, J. H. Mentink, M. I. Katsnelson, T. Rasing, A. Kirilyuk, A. Kimel, O. Eriksson, and M. Pereiro, All-thermal switching of amorphous Gd-Fe alloys: Analysis of structural properties and magnetization dynamics, *Phys. Rev. B* **92**, 094411 (2015).
- [30] J. Barker, U. Atxitia, T. A. Ostler, O. Hovorka, O. Chubykalo-Fesenko, and R. W. Chantrell, Two-magnon bound state causes ultrafast thermally induced magnetization switching, *Sci. Rep.* **3**, 3262 (2013).
- [31] Z. Lin, L. V. Zhigilei, and V. Celli, Electron-phonon coupling and electron heat capacity of metals under conditions of strong electron-phonon nonequilibrium, *Phys. Rev. B* **77**, 075133 (2008).
- [32] T. Zhou, Coupled Interactions of Multiple Laser Beam and Novel Surface Ablation Phenomena Through Spatial Light Modulation, Ph.D. thesis, The University of Liverpool, 2021, p. 127.
- [33] F. Steinbach, U. Atxitia, K. Yao, M. Borchert, D. Engel, F. Bencivenga, L. Foglia, R. Mincigrucci, E. Pedersoli, D. De Angelis *et al.*, Exploring the fundamental spatial limits of magnetic all-optical switching, *Nano Lett.* **24**, 6865 (2024).